Cotunneling Drag Effect in Coulomb-Coupled Quantum Dots

A. J. Keller,[1,*] J. S. Lim,[2] David Sánchez,[3] Rosa López,[3] S. Amasha,[1,†] J. A. Katine,[4]
Hadas Shtrikman,[5] and D. Goldhaber-Gordon[1,‡]

[1]*Department of Physics, Stanford University, Stanford, California 94305, USA*
[2]*School of Physics, Korea Institute for Advanced Study, Seoul 130-722, Korea*
[3]*IFISC (UIB-CSIC), E-07122 Palma de Mallorca, Spain*
[4]*HGST, San Jose, California 95135, USA*
[5]*Department of Condensed Matter Physics, Weizmann Institute of Science, Rehovot 96100, Israel*
(Received 29 February 2016; published 4 August 2016)

In Coulomb drag, a current flowing in one conductor can induce a voltage across an adjacent conductor via the Coulomb interaction. The mechanisms yielding drag effects are not always understood, even though drag effects are sufficiently general to be seen in many low-dimensional systems. In this Letter, we observe Coulomb drag in a Coulomb-coupled double quantum dot and, through both experimental and theoretical arguments, identify cotunneling as essential to obtaining a correct qualitative understanding of the drag behavior.

Coulomb-coupled quantum dots yield a model system for Coulomb drag [1], the phenomenon where a current flowing in a so-called drive conductor induces a voltage across a nearby drag conductor via the Coulomb interaction [2]. Though charge carriers being dragged along is an evocative image, as presented in early work on coupled 2D-3D [3] or 2D-2D [4] semiconductor systems, later measurements in graphene [5,6], quantum wires in semiconductor 2DEGs [7–10], and coupled double quantum dots [11] have indicated that the microscopic mechanisms leading to Coulomb drag can vary widely. For example, collective effects are important in 1D, but less so in other dimensions. All drag effects require interacting subsystems and vanish when both subsystems are in local equilibrium.

A perfect Coulomb drag with equal drive and drag currents has been observed in a bilayer 2D electron system: effectively a transformer operable at zero frequency [12]. Coulomb-coupled quantum dots can rectify voltage fluctuations to unidirectional current, with possible energy harvesting applications [13,14]. This rectification of nonequilibrium fluctuations is similar to a ratchet effect, as observed in charge- [15–18] and spin-based nanoelectronic devices [19], as well as in rather different contexts such as suspended colloidal particles in asymmetric periodic potentials [20]. Coulomb-coupled dots have also been proposed as a means for testing fluctuation relations out of equilibrium [1].

An open question is how higher-order tunneling events in the quantum coherent limit contribute to Coulomb drag processes [21]. In this Letter, we present experimental measurements and theoretical arguments showing that simultaneous tunneling of electrons (cotunneling) is crucial to describe drag effects qualitatively in Coulomb-coupled double quantum dots (CC-DQDs). Previous theoretical work has obtained drag effects with sequential tunneling models [1] (for an exception, see Ref. [22]), and these models have been invoked in measurements of stacked graphene quantum dots [21]. We demonstrate here that for a DQD, cotunneling contributes to the drag current at the same order as sequential tunneling in a perturbation expansion. This has profound consequences in experiment, notably a measurable drag current even when the drag dot is far off resonance, and a gate voltage-dependent vanishing of the Coulomb gap above which the drag current can be measured. Our experiment shows that the drag mechanisms considered can be observed in highly tunable GaAs/AlGaAs QDs, not only in graphene. We also achieve the unexplored regime $kT \ll \hbar\Gamma$, where T is temperature and Γ is a tunnel rate, which is outside the scope of theories to date.

Our device [Fig. 1(a)] consists of a lithographically patterned AlGaAs/GaAs heterostructure with electron density 2×10^{11} cm^{-2} and mobility 2×10^{6} cm^{2}/V s. All measurements are taken in a dilution refrigerator.
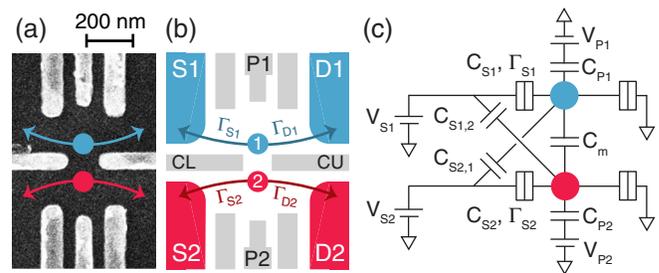

FIG. 1. Device and model. (a) Top-down SEM image of a device nominally identical to that measured. Ti/Au gate electrodes (light gray) are patterned on the substrate surface (dark gray). Colored circles represent the QDs. Arrows indicate where electrons can tunnel. (b) Cartoon showing names of gates, reservoirs, and dots. Γ_{Si} is the tunnel rate between reservoir Si and dot i. (c) Capacitor and tunnel junction network. Interdot tunneling is strongly suppressed and not included in the model. Direct capacitance between gate P1 (2) and dot 2 (1) is omitted from the diagram for clarity, along with some labels.

The interdot tunnel rate is made negligible, tens of times smaller than all other dot-lead tunnel rates, by applying appropriate voltages on gate electrodes named CL and CU [Fig. 1(b)], as done previously with the very same device [23,24]. The device then realizes a capacitance and tunnel junction network sufficient to observe Coulomb drag [Fig. 1(c)] [1]. We measure $G_i = dI_i/dV_{Si}$ and I_i for dot $i \in \{1, 2\}$, using standard current preamp+lock-in amplifier techniques. The near-dc current measurements of I_i were obtained by filtering current amplifier outputs with single-stage low-pass filters ($R = 2.7$ kΩ, $C = 10$ μF). In all measurements we present in this paper an in-plane field of 2.0 T and an out-of-plane field of 0.1 T were applied. The application of a small out-of-plane field can help tune couplings. The large in-plane field breaks spin degeneracy of the dot levels to simplify the discussion. The magnetic field is not necessary to observe drag currents.

For zero source-drain bias, peaks in measured $G_i = dI_i/dV_{Si}$ correspond to charge transitions of the dots [Fig. 2(a)]. The measured, summed conductance $G_1 + G_2$ shows both charge transitions [Fig. 2(b)]. By a change of basis from the gate voltage axes V_{P1} and V_{P2}, we measure along the dot level axes $-\varepsilon_1$ and $-\varepsilon_2$. The dots can be Coulomb blockaded as both temperature T and the dot-lead tunnel rates $\Gamma_i = \Gamma_{Si} + \Gamma_{Di}$ are small compared to the addition energies U_i. The numbers of electrons on the dots are unknown in this experiment, but we can label how many there are relative to some (N, M) in Fig. 2(b). By taking horizontal or vertical cuts on the bottom or left edges of Fig. 2(b), respectively, we extract the FWHM of the observed peaks and find $\Gamma_1 = 15$ μeV and $\Gamma_2 = 47$ μeV, considerably larger than $T = 20$ mK ≈ 1.7 μeV. Quantum coherent processes may therefore be important.

When applying a source-drain bias V_{S1} (V_{D1} is fixed at zero), a window in $-\varepsilon_1$ should open wherein peaks in G_1, reflecting excited states of dot 1, may be observed [Fig. 2(a)]. The location of this window depends on $-\varepsilon_2$; we define three regions to aid in discussion. In Fig. 2(c), we apply $V_{S1} = 0.5$ mV and see excited states, e.g., between $-\varepsilon_1 = 0$ and $|e|V_{S1}$ in region (i), or between $-\varepsilon_1 = U$ and $|e|V_{S1} + U$ in region (iii), where U is the interdot charging energy [25]. For ε_1, ε_2 within any shaded region of Fig. 2(a), the measured G_1 is accompanied by a nonzero dc current I_1 that can drive Coulomb drag.

Keeping $V_{S1} = 0.5$ mV, and noting that both reservoirs S2 and D2 are grounded, we easily resolve a drag current $I_2 \sim 40$ pA in region (ii) [Fig. 2(e)]. More surprisingly, we still see significant I_2 in region (iii), where sequential tunneling in dot 2 should be very suppressed, with the current decreasing as $-\varepsilon_2$ grows. Current on the order of 0.5 pA is also measured in region (i), decreasing as $-\varepsilon_2$ decreases. G_2 is apparently insensitive to the current flowing in dot 1 in regions (i,iii) [Fig. 2(d)]. Upon inverting the sign of V_{S1}, we observe qualitatively similar features in
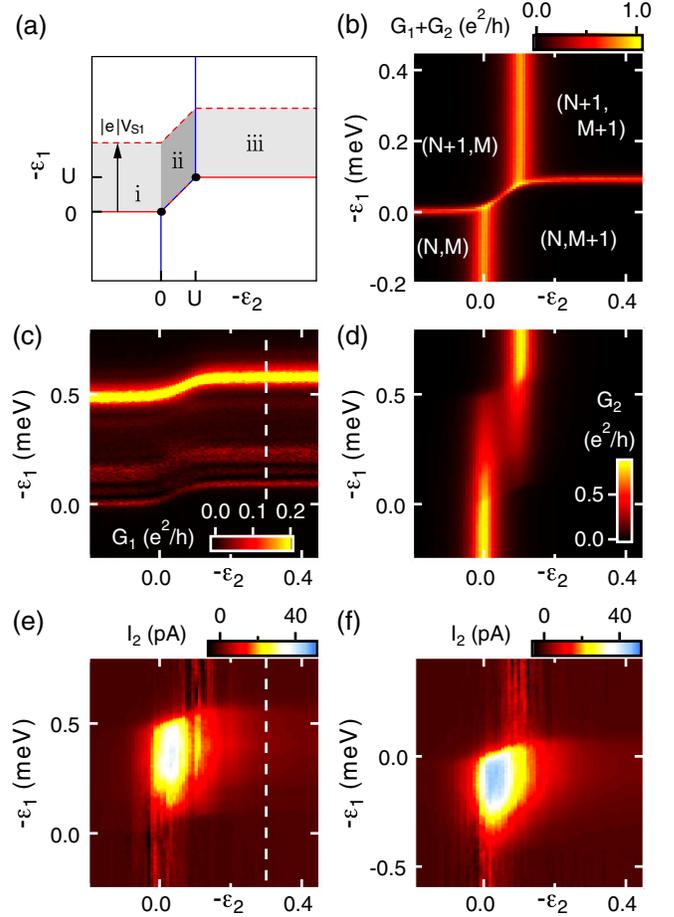

FIG. 2. Coulomb drag. (a) Schematic charge stability diagram for a CC-DQD. Dots indicate triple points. Red (blue) solid lines are charge transitions for dot 1 (2). As V_{S1} increases from zero, excited states appear in G_1 within shaded regions. Roman numerals are used later for reference. (b) Sum of measured conductances $G_i = dI_i/dV_{Si}$ for $V_{S1} = V_{S2} = 0$, as a function of dot levels ε_1, ε_2. (c),(d) Measured G_1 (c) and G_2 (d) for $V_{S1} = 0.5$ mV. (e),(f) Measured I_2 for $V_{S1} = 0.5$ mV (e) and $V_{S1} = -0.5$ mV (f). In both cases the current I_2 flows in the same direction, is strongest in region (ii), and persists in regions (i) and (iii). Dashed white lines in (c) and (e) are discussed in the text.

I_2 [Fig. 2(f)]. The drag current flows in the same direction, regardless of V_{S1}'s sign. Vertical cuts in Figs. 2(c) and 2(e) are compared in Sec. E of Ref. [26] and indicate sensitivity of I_2 to dot 1's excited states.

Having demonstrated Coulomb drag, we perform bias spectroscopy (Fig. 3) to detect the presence of a Coulomb gap—an energy below which drag currents are vanishing—as indicated in prior theoretical studies of drag in CC-DQDs [1]. For $-\varepsilon_2$ on the border of region (ii) and (iii) of Fig. 2(a), such a gap does not clearly appear. Figures 3(a) and 3(b) show G_1 and I_2, respectively, and a nonzero current I_2 flows provided $0.1 < -\varepsilon_1 < 0.1 + |e|V_{S1}$. Current noise is intrinsically strong for this tuning of $-\varepsilon_2$, as also seen in Figs. 2(e) and 2(f). However, if $-\varepsilon_2$ is well within region (iii) of Fig. 2(a), there appears to be a gap.
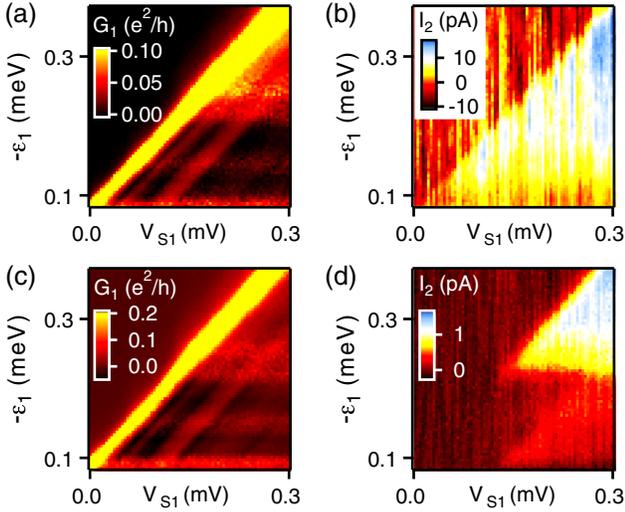
(a) G_1 (e^2/h)

(b) I_2 (pA)

(c) G_1 (e^2/h)

(d) I_2 (pA)

FIG. 3. For small drive bias V_{S1}, the drag current I_2 appears to vanish depending on the drag dot's level. (a) G_1 for $-\varepsilon_2 = 0.12$ meV, on the border of region (ii) and (iii) in Fig. 2(a). The color scale is saturated to emphasize fine features. (b) Drag current I_2 for $-\varepsilon_2 = 0.12$ meV persists even in the limit that drive bias $V_{S1} \to 0$. (c) G_1 for $-\varepsilon_2 = 0.47$ meV, well within region (iii) in Fig. 2(a). The color scale is saturated, and appears similar to (a). (d) I_2 for $-\varepsilon_2 = 0.47$ meV (region (iii)). Below $V_{S1} \sim 0.12$ meV, the drag current is unmeasurable. This gap also appears for $-\varepsilon_1 < 0.1$ and negative V_{S1} (not shown), and is the same value within measurement accuracy.

[Figs. 3(c) and 3(d)]. Though G_1 looks similar to before, I_2 looks dramatically different, with much less current noise, smaller average drag currents, and a gap of ~0.12 meV. The range of (V_{S1}, $-\varepsilon_1$) where drag current flows appears to be bounded by excited states seen in Fig. 3(c). The size of the gap does not seem to depend on $-\varepsilon_2$ in region (iii); we have verified this for $-\varepsilon_2 \in \{0.21, 0.29, 0.38\}$. At each of these values, I_2 looks much like it does in Fig. 3(d), but with different magnitude. We note the observed gap of 0.12 meV is close to $U \sim 0.1$ meV.

To elucidate the mechanisms behind the Coulomb drag, we study the T and $-\varepsilon_2$ dependence of I_2. Changing the temperature has a weak effect if any in the range 20 to 155 mK, in both regions (ii) [Fig. 4(a), top] and (iii) [Fig. 4(a), bottom]. Our electron temperature determination is based on calibrating a ruthenium-oxide resistive thermometer in the mixing chamber of our dilution refrigerator to Coulomb blockade thermometry measurements performed in equilibrium. As such, we cannot rule out the possibility that our base electron temperature is higher than 20 mK in the presence of large biases. The $-\varepsilon_2$ dependence shows that a drag current is measurably large for *any* value of $-\varepsilon_2$ [Fig. 4(b)]. For small biases, prior theories with sequential tunneling only [1] would yield vanishingly small drag currents if the dot levels were off resonance by more than the width of the Fermi-Dirac distribution.
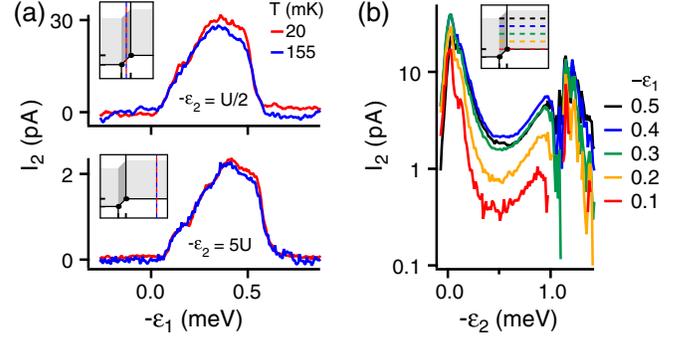

FIG. 4. Temperature and dot level dependence of drag current. Icons indicate where cuts are taken (as in Fig. 2(a)). $V_{S1} = 500$ μV, $V_{S2} = 0$. (a) Temperature-dependent I_2. Top: $-\varepsilon_2 = 0.05$ meV $= U/2$ (middle of region (ii) in Fig. 2(a)); bottom: $-\varepsilon_2 = 0.5$ meV $= 5U$ (deep in region (iii)]. The drag current does not change appreciably from 20 to 155 mK in either case. (b) Drag current I_2 can be measured even when dot 2's levels are far off resonance, provided a current is flowing in dot 1.

We now show that the interpretation of our data is compatible with a theoretical model that includes both sequential and cotunneling processes. Remarkably, we find here that sequential and cotunneling processes contribute to the drag current to the same order despite the cotunneling rate being calculated from a higher-order perturbative term. This is illustrated in Fig. 5: while a sequential drag current needs four hoppings in four steps [Fig. 5(a)], a pure cotunneling current requires only two steps [Fig. 5(b)]. Therefore, a complete theory of the drag effect in CC-DQD must take into account both types of processes on equal footing. We discuss our results on the basis of a master equation approach. From Fig. 2(b) we consider four charge states in the CC-DQD system: $\{|0\rangle = |00\rangle, |1\rangle = |10\rangle, |2\rangle = |01\rangle, |d\rangle = |11\rangle\}$. The set of stationary probabilities that the system is in any of these states obeys the kinetic equations $0 = \mathbf{\Gamma p}$, where $\mathbf{p} = (p_0, p_1, p_2, p_d)^T$ fulfills $p_0 + p_1 + p_2 + p_d = 1$ and $\mathbf{\Gamma}$ denotes the matrix containing the rates. A representative equation reads

$$0 = \Gamma_{10}p_1 + \Gamma_{20}p_2 + \gamma_{d0}p_0 - (\Gamma_{02} + \Gamma_{01} + \gamma_{0d})p_0. \quad (1)$$

(The remaining equations are shown in Sec. D of Ref. [26].) Here, $\Gamma_{0i(i0)} = \sum_\alpha \Gamma_{0i(i0)}^{\alpha i}$ and $\gamma_{0d(d0)} = \sum_{\alpha,\beta} \gamma_{0d(d0)}^{\alpha 1\beta 2}$. $\Gamma_{0i(i0)}^{\alpha i}$ is the sequential rate that describes the addition (removal) of an electron into (from) dot $i = 1, 2$ from (to) lead αi with $\alpha = S, D$ and $\gamma_{0d(d0)}^{\alpha 1\beta 2}$ is the cotunneling rate that characterizes the simultaneous tunneling of two electrons on (off) the CC-DQD with $\beta = S, D$. The expressions for these rates follow from a perturbation expansion in the tunneling coupling [28], valid for $kT > \Gamma$. To lowest order one finds $\Gamma_{0i}^{\alpha i} = (\Gamma_{\alpha i}/\hbar)f_{\alpha i}(\mu_i)$ and $\Gamma_{i0}^{\alpha i} = (\Gamma_{\alpha i}/\hbar)[1 - f_{\alpha i}(\mu_i)]$ with $\Gamma_{\alpha i}$ the level broadening of dot i due to hybridization with lead αi, $f_{\alpha i}(x) = 1/[1 + e^{(x-\mu_{\alpha i})/kT}]$ the Fermi-Dirac distribution function ($\mu_{\alpha_i} = E_F + eV_{\alpha i}$) and μ_i the electrochemical potential of dot i. This has to be determined from
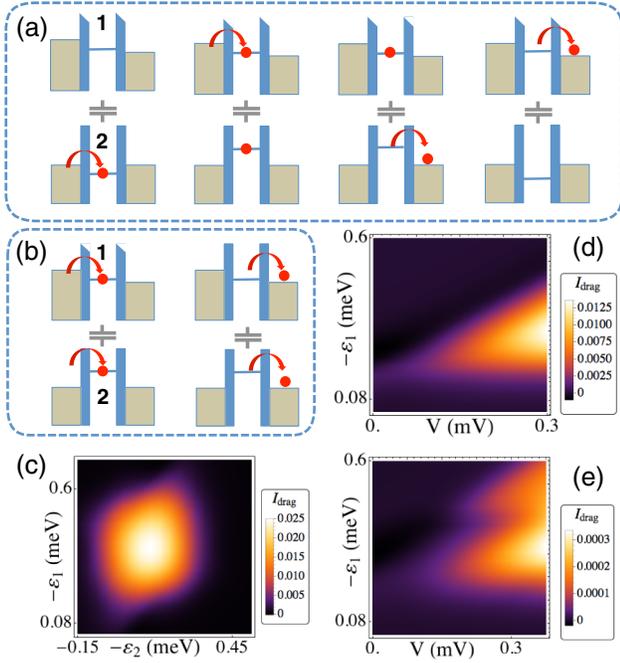
FIG. 5. Theory of cotunneling leading to drag. (a) Illustration of a sequential process leading to drag current. An electron hops into the drag dot (dot 2). Next, an electron hops into the drive dot (dot 1), causing the dot 2 level to rise due to interdot Coulomb repulsion in turn allowing the electron in 2 to be transferred to the right. The whole process involves four tunneling rates and is hence of order Γ^4. (b) Pure cotunneling process leading to drag current. Two electrons tunnel simultaneously onto the dots. They then tunnel off simultaneously. Since each cotunneling process has a probability Γ^2, the cotunneling drag process is of order Γ^4 as in (a). (c) Calculated drag current in units of $e\Gamma/\hbar$ for drive voltage $V = 0.5$ mV and system parameters extracted from the experiment. (d),(e) Drag current as a function of drive dot level and V for (d) $\varepsilon_2 = -0.2$ meV and (e) $\varepsilon_2 = -0.4$ meV.

an electrostatic model that takes into account both the polarization charges due to electric shifts in the leads [C_{Si} in Fig. 1(c)] and the interdot electron-electron interaction [C_m in Fig. 1(c)]. The cotunneling rates [Fig. 5(b)] are found in the next order in the tunneling coupling,

$$\gamma_{0d}^{\bar{\alpha i}\beta i} = \frac{2\pi}{\hbar} \int d\varepsilon \left| \frac{t_{\alpha i}^0 t_{\beta i}^1}{\varepsilon - \mu_{\bar{i}} + i\eta} - \frac{t_{\alpha i}^1 t_{\beta i}^1}{\varepsilon - \mu_{\bar{i}} - U + i\eta} \right|^2$$
$$\times \rho_{\alpha \bar{i}} \rho_{\beta i} f_{\alpha \bar{i}}(\varepsilon) f_{\beta i}(\mu_i + \mu_{\bar{i}} + U - \varepsilon), \quad (2)$$

where $\bar{i} = 2(1)$ if $i = 1(2)$, U is given by a combination of the system capacitances, ρ is the lead density of states, and a small imaginary part $\eta \to 0^+$ is added to avoid the divergence due to the infinite lifetime of the virtual intermediate states [29,30]. $\gamma_{d0}^{\bar{\alpha i}\beta i}$ is found by replacing f with $(1 - f)$ in Eq. (2). Importantly, $t_{\alpha i}^0$ ($t_{\beta i}^1$) is the tunneling amplitude for barrier αi (βi) when zero (one) charges are present in the DQD. That the amplitudes depend on the charge state derives physically from the general fact that

tunneling is energy dependent and the dot levels shift with the charge state according to the electrostatic model. This is a crucial condition to generate drag currents. The probability that the sequence $|0\rangle \to |2\rangle \to |d\rangle \to |1\rangle \to |0\rangle$ drags an electron from left to right [Fig. 5(a)] must differ from the reverse sequence. This occurs only if Γ is energy dependent, for both sequential [1] and cotunneling processes.

The drag current is given by $I_{\text{drag}} \equiv I_{S2} = e[\Gamma_{20}^{S2}p_2 + \Gamma_{d1}^{S2}p_d - \Gamma_{02}^{S2}p_0 - \Gamma_{d1}^{S2}p_1 + \sum_\alpha \gamma_{21}^{\alpha1S2}p_2 + \sum_\alpha \gamma_{d0}^{\alpha1S2}p_d - \sum_\alpha \gamma_{0d}^{S2\alpha1}p_0 - \sum_\alpha \gamma_{12}^{S2\alpha1}p_1]$ (we take $\mu_{S2} = \mu_{D2}$). We extract the parameters from the experiment and plot the results in Fig. 5(c) for a drive voltage $V = 0.5$ mV [31]. Comparing with the data in Fig. 2(e) we obtain a good agreement. We find in Fig. 5(c) an extended region of nonzero drag current as compared to the sequential case [1], although the size of this region observed in Fig. 2(e) is even larger than predicted, probably due to increased coherence in the experiment at lower T.

In Fig. 3(b) we saw no Coulomb gap. The theoretical dependence of I_{drag} with V [Fig. 5(d)] reproduces this observation, in stark contrast to the theory of Ref. [1], further emphasizing the role of cotunneling. Physically, transport can occur via nonlocal cotunneling processes ($|1\rangle \to |2\rangle$ or vice versa) without traversing the doubly occupied state $|d\rangle$, so the Coulomb gap disappears. For a larger value of $|\varepsilon_2|$ the gap reappears [Fig. 5(e)] in agreement with the experiment [Fig. 3(d)].

In conclusion, cotunneling is essential to understanding drag effects in CC-DQDs. We extend the existing theoretical framework to account for cotunneling processes, which cannot be justifiably neglected, as seen in experimental data. Though the theoretical framework is only valid for high temperatures, we are encouraged by the qualitative agreement between experiment and theory. Explaining some features in the experiment—namely the apparently weak temperature dependence and the role of excited states—will require additional theory. Double quantum dots are a popular model system for many-body physics, and play important roles in quantum information. Understanding the subtle transport mechanisms in double quantum dots may thus have broad implications.

*Present address: Institute for Quantum Information and Matter, California Institute of Technology, Pasadena, California 91125, USA.

[†]Present address: MIT Lincoln Laboratory, Lexington, Massachusetts 02420, USA.

[‡]goldhaber-gordon@stanford.edu

[1] R. Sánchez, R. López, D. Sánchez, and M. Büttiker, Phys. Rev. Lett. **104**, 076801 (2010).

[2] B. N. Narozhny and A. Levchenko, Rev. Mod. Phys. **88**, 025003 (2016).

[3] P. M. Solomon, P. J. Price, D. J. Frank, and D. C. La Tulipe, Phys. Rev. Lett. **63**, 2508 (1989).

[4] T. J. Gramila, J. P. Eisenstein, A. H. MacDonald, L. N. Pfeiffer, and K. W. West, Phys. Rev. Lett. **66**, 1216 (1991).

[5] S. Kim, I. Jo, J. Nah, Z. Yao, S. K. Banerjee, and E. Tutuc, Phys. Rev. B **83**, 161401 (2011).

[6] R. V. Gorbachev, A. K. Geim, M. I. Katsnelson, K. S. Novoselov, T. Tudorovskiy, I. V. Grigorieva, A. H. MacDonald, S. V. Morozov, K. Watanabe, T. Taniguchi, and L. A. Ponomarenko, Nat. Phys. **8**, 896 (2012).

[7] P. Debray, V. Zverev, O. Raichev, R. Klesse, P. Vasilopoulos, and R. S. Newrock, J. Phys. Condens. Matter **13**, 3389 (2001).

[8] M. Yamamoto, M. Stopa, Y. Tokura, Y. Hirayama, and S. Tarucha, Science **313**, 204 (2006).

[9] D. Laroche, G. Gervais, M. P. Lilly, and J. L. Reno, Nat. Nanotechnol. **6**, 793 (2011).

[10] D. Laroche, G. Gervais, M. P. Lilly, and J. L. Reno, Science **343**, 631 (2014).

[11] G. Shinkai, T. Hayashi, T. Ota, K. Muraki, and T. Fujisawa, Appl. Phys. Express **2**, 081101 (2009).

[12] D. Nandi, A. D. K. Finck, J. P. Eisenstein, L. N. Pfeiffer, and K. W. West, Nature (London) **488**, 481 (2012).

[13] F. Hartmann, P. Pfeffer, S. Höfling, M. Kamp, and L. Worschech, Phys. Rev. Lett. **114**, 146805 (2015).

[14] H. Thierschmann, R. Sánchez, B. Sothmann, F. Arnold, C. Heyn, W. Hansen, H. Buhmann, and L. W. Molenkamp, Nat. Nanotechnol. **10**, 854 (2015).

[15] H. Linke, T. E. Humphrey, A. Löfgren, A. O. Sushkov, R. Newbury, R. P. Taylor, and P. Omling, Science **286**, 2314 (1999).

[16] E. Onac, F. Balestro, L. H. Willems van Beveren, U. Hartmann, Y. V. Nazarov, and L. P. Kouwenhoven, Phys. Rev. Lett. **96**, 176601 (2006).

[17] V. S. Khrapai, S. Ludwig, J. P. Kotthaus, H. P. Tranitz, and W. Wegscheider, Phys. Rev. Lett. **97**, 176803 (2006).

[18] B. Roche, P. Roulleau, T. Jullien, Y. Jompol, I. Farrer, D. A. Ritchie, and D. C. Glattli, Nat. Commun. **6** (2015).

[19] M. V. Costache and S. O. Valenzuela, Science **330**, 1645 (2010).

[20] J. Rousselet, L. Salome, A. Ajdari, and J. Prostt, Nature (London) **370**, 446 (1994).

[21] D. Bischoff, M. Eich, O. Zilberberg, C. Rössler, T. Ihn, and K. Ensslin, Nano Lett. **15**, 6003 (2015).

[22] K. Kaasbjerg and A.-P. Jauho, Phys. Rev. Lett. **116**, 196801 (2016).

[23] S. Amasha, A. J. Keller, I. G. Rau, A. Carmi, J. A. Katine, H. Shtrikman, Y. Oreg, and D. Goldhaber-Gordon, Phys. Rev. Lett. **110**, 046604 (2013).

[24] A. J. Keller, S. Amasha, I. Weymann, C. P. Moca, I. G. Rau, J. A. Katine, H. Shtrikman, G. Zárand, and D. Goldhaber-Gordon, Nat. Phys. **10**, 145 (2014).

[25] Note that we apply V_{S1} while compensating with gate voltages V_{P1}, V_{P2} to avoid changing either of the dot levels, though the ac part of the bias may still act as an ac gate.

[26] See Supplemental Material at http://link.aps.org/supplemental/10.1103/PhysRevLett.117.066602 for additional data and further theoretical details, which includes Ref. [27].

[27] W. G. Van der Wiel, S. De Franceschi, J. M. Elzerman, T. Fujisawa, S. Tarucha, and L. P. Kouwenhoven, Rev. Mod. Phys. **75**, 1 (2002).

[28] H. Bruus and K. Flensberg, *Many-Body Quantum Theory in Condensed Matter Physics* (Oxford University Press, Oxford, England, 2004).

[29] D. Averin, Physica (Amsterdam) **194B–196B**, 979 (1994).

[30] M. Turek and K. A. Matveev, Phys. Rev. B **65**, 115332 (2002).

[31] The only different parameter is temperature. We take $k_B T = 5\Gamma$ to ensure the validity of our theory. Note that the experiments show a weak dependence of I_{drag} with $k_B T$ [Figs. 4(a) and (b)].